Title

Field Implementation of a Real-time Battery Control Scheme for a Microgrid at the University of California, Riverside

Permalink

https://escholarship.org/uc/item/8kk0f2w8

Authors

Xue, Yun
Todd, Michael
Ula, Sadrul
<u>et al.</u>

Publication Date

2019-05-01

Peer reviewed

Field Implementation of a Real-time Battery Control Scheme for a Microgrid at the University of California, Riverside

Yun Xue
Department of Electrical Engineering
University of California, Riverside
Riverside, US

Michael Todd, Sadrul Ula, Alfredo Martinez-Morales
Center for Environmental Research & Technology
University of California, Riverside
Riverside, US

Abstract—**This study demonstrates a real-time battery control scheme which consists of off-peak, mid-peak and on-peak period operation of a microgrid system at the University of California, Riverside. Using limited system historical information, the control scheme minimizes demand peak and energy consumption from the grid under a time of use (TOU) rate schedule. The off-peak operation mode fully charges the battery system while keeping low building demand by autonomously adjusting the demand threshold based on the real-time building load. The mid-peak operation mode maximizes self-consumption of onsite renewable energy by consuming surplus energy stored in the battery system. As previous reported, on-peak operation mode minimizes the building net load by optimally discharging the battery system based on real-time solar generation and building load consumption.**

Index Terms-- **battery energy management system, demand peak reduction, load shifting, microgrid.**

I. INTRODUCTION

It has been reported that centralized power plants can negatively affect the environment in many ways, such as the emission of air pollutants, and affecting land use. Furthermore, centralized generation has the inherent drawback of high energy losses associated with transmission and distribution [1]. In contrast, on-site, distributed renewable energy generation offers a path forward without the aforementioned drawbacks. One common approach to manage distributed energy resources (DERs) assets is through a microgrid system, which incorporates the distributed generation and associated electrical loads within a localized power grid. The microgrid architecture, characterized by a local energy management system (EMS), reduces (and some cases eliminates) the need for central dispatch [2]. Microgrid projects are expanding rapidly worldwide. The California's renewables portfolio standard provides a major impetus for microgrid development, which has a target of obtaining 50% of the state's electricity from eligible renewable resources by 2030, 100% zero net-energy buildings by 2020 for all new residential buildings and for all new commercial buildings by 2030 [3].

In 2014, University of California – Riverside launched the Sustainable Integrated Grid Initiative (SIGI), one of the largest renewable energy initiatives of its kind in the state.

Fig.1 illustrates the actual microgrid system which includes a 500 kW of solar generation, 100 kW/500 kWh stationary battery energy storage system (BESS), 100 kW/ 500 kWh mobile BESS (installed in a trailer), and three facility buildings. This study is performed and implemented by using a sub-portion of the SIGI microgrid, comprised of a 100 kW solar PV system, 100 kW/500 kWh stationary battery, and one research laboratory building with highly variable equipment loads of laboratory experiments during working hours. The electric tariff for the building is Riverside Public Utility's (RPU's) large general and industrial service, time of use (TOU) rate schedule. In addition to fix charges, the monthly TOU rate schedule charges consist of two components: demand charges ($/kW) and energy use charges ($/kWh). There are three TOU periods, off-peak, mid-peak and on-peak which change between summer and winter season [4], where off-peak has the lowest price rate and the on-peak has the highest price rate.

Generally, well-documented meteorological information and long-term historical trends are required for establishing accurate prediction models for solar generation and building loads [5,6]. In practice, building sophisticated prediction models is often hindered by the ease of access by end-users to comprehensive data sets. This challenge is augmented by the different demand charges during one billing cycle that require further consideration for minimizing peak demand across multiple rate periods, which is an aspect of demand charge management that is regularly ignored in the literature.

The goal of this study, however, is to design and perform a real-time battery control scheme for the SIGI microgrid where only basic information such as real-time building load, solar power generation, and short-term historical data are available. The proposed control scheme employing three different operations strategies, one for each rate periods is to: 1) shift the grid electricity from the high consumption time to low consumption time, 2) reduce the peak demand for different rate periods, and 3) efficiently utilize the BESS to store and deliver energy. This advanced and easy implementation real-time battery control scheme can increase the system economic benefit without adding the complexity of the microgrid system, which has achieved significant electricity cost savings for the SIGI microgrid.
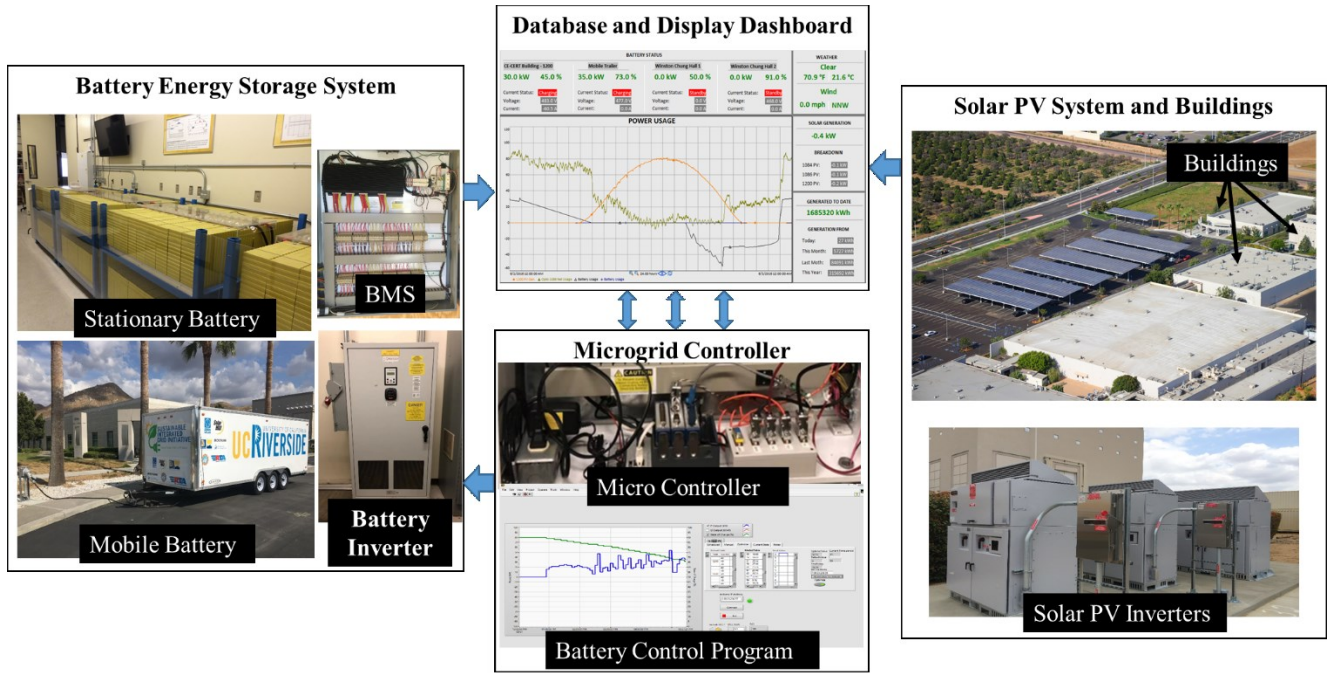
Figure 1. SIGI Microgrid System Architeture and Data Flow

II. INTRODUCTION TO THE REAL-TIME BATTERY CONTROL SCHEME

To efficiently manage fluctuating peak demand under the TOU rate schedule, the developed battery control scheme consists of three battery operational modes for each of the three different rate periods. The battery charging and discharging process is modeled as a linear process from the field experiments. To prolong the useful life span of the BESS, charging and discharging is constraint within 40% to 90% state of charge (SOC) [7]. A lower limit of a 20% SOC is allowed only when the microgrid needs to provide higher amount of energy due to situation where solar generation is too low and/or the building electrical load is too high.

The peak demand is calculated over a 15-minute moving average by the utility revenue meter. For implementing real-time control with consideration for the limitations posed by the net metering devices installed on the site and the 15-minute demand window, the horizon for each control time slot is set to be 5 minutes.

A. Off-Peak Operation: Adjusting Off-Peak Threshold

During working days, the off-peak rate period is from 23:00 to 08:00 in the summer time, and from 22:00 to 08:00 in the winter time. Weekends and holidays during the entire year are considered off-peak period. The control objectives during off-peak battery operation are: 1) charging the BESS to 90% SOC, and 2) maintaining a low off-peak demand value. The off-peak threshold *offSch*, is predetermined by the previous months' off-peak load demand, which limits the off-peak demand. In most cases, the BESS maintains a stable charging power and does not exceed the *offSch* due to low and stable electricity consumption. When the electricity load consumption is high, an autonomous adjustment of *offSch* is

achieved by tracking the SOC difference between the desired and the actual charging power.

The off-peak rate period is divided into M_{off} slots. In summer season, $M_{off} = 102$ (23:15 − 7:45), and in winter season, $M_{off} = 114$ (21:15 − 7:45). The principles of off-peak battery operation can be described as follows:

(i) At i = 0, set off-peak control horizon M_{off}, predetermined off-peak demand *offSch*, $\Delta soc = 0$; Δt is the control slot which is 5 minutes: $\Delta t = 5/60$;

(ii) At time $i = k$, fetch the most current system data:

$Pnet_i$: net load; Ps_i: solar generated power; Pl_i: building electrical load; SOC_i: state of charge of the BESS; bc_i: battery capacity; bp_{i-1}: last 5-minute battery operational power, where

$$Battery\ is \begin{cases} charging, & bp_i < 0 \\ discharging, & bp_i \geq 0 \end{cases}$$

$$Pnet_i = Pl_i - Ps_i - bp_i$$

Calculate the desired charging power

$$pca_i \tag{1}$$
$$= -\min\left(\frac{\frac{SOC_{max} - SOC_i}{100} \cdot bmax}{(M_{off} - i + 1) \cdot \Delta t}, 100\right)$$

The battery inverter is rated at 100 kW; therefore, the maximum charge power is -100 kW.

(iii) The actual charging power

$$bp_i = \begin{cases} 0, & Pl_i - Ps_i > offSch \\ offSch - Pl_i + Ps_i, & Pl_i - Ps_i + pca_i > offSch \\ & \cap \Delta soc < 0 \\ pca_i, & else \end{cases}$$

(iv) Update Δsoc

$$\Delta soc = (pca_i - bp_i) \cdot \Delta t + \Delta soc \qquad (2)$$

(v) If $\Delta soc < -0.5$, Update $offSch$

$$offSch = offSch + 2.5$$
$$\Delta soc = 0$$

(vi) Set $i = k + 1$; then go back to step (ii) until $i = M_{off}$ or $SOC = 90$.

B. Mid-Peak Operation

During winter, the mid-peak rate period is from 08:00 to 17:00, while during summer season it is between 08:00 to 12:00 and 18:00 to 23:00. During winter, the mid-peak period overlaps with normal business working hours of the facility and much of the solar generation can be used to support the building's electricity consumption. Additionally, the BESS can be fully utilized towards supporting on-peak period energy consumption after sunset. Therefore, during mid-peak period in winter, the control system only monitors the system operating in a passive mode. In the summer time, the following control algorithm is used: for the first mid-peak period from 08:00 to noon, 10% of the battery capacity (from 90% to 80% SOC) is allowed to be discharged during this time to avoid high mid-peak demand. For the second mid-peak period (18:00 to 23:00), the remaining battery capacity left from the on-peak rate period, is uniformly distributed over this period. In the events of excessive building load, the controller determines the discharge rate needed to maintain the predetermined mid-peak demand $midSch$. In the second mid-peak period, the battery is allowed to discharge down to 20% SOC in certain circumstances.

The summer mid-peak period is divided into two parts, $M_{1mid} = 48$ (07:45 – 11:45) and $M_{2mid} = 60$ (18:15 – 23:15). The first mid-peak operation principles can be described as follows:

(i) At $i = 0$, set mid-peak control horizon M_{1mid}, and retrieve the scheduled mid-peak demand $midSch$;

(ii) At $i = k$, fetch the most current system data: Ps_i, Pl_i, bc_i, bp_{i-1}, $Pnet_i$, SOC_i;

(iii) If $SOC_i \geq 80$ and $Pnet_i > midSch$, activate discharging process based on the current system status:

$$bp_i = \begin{cases} Pnet_i - (midSch - 5), & discharging \\ & when\ SOC_i \geq 80 \cap Pnet_i > midSch \\ Pnet_i - (midSch - 10), & charging \\ & when\ SOC_i < 90 \cap Pnet_k \leq midSch - 10 \\ 0, & idle\ when\ else \end{cases}$$

(iv) Update $midSch$;

(v) Set $i = k + 1$; then go back to (ii) until $i = M_{1mid}$.

The second mid-peak operation principles can be summarized as follows:

(i) At $i = 0$, set mid-peak control horizon M_{2mid}, retrieve the scheduled mid-peak demand $midSch$;

(ii) At $i = k$, fetch the most current system data: Ps_i, Pl_i, bc_i, bp_{i-1}, SOC_i;

(iii) If $SOC_i > 40$, calculate the average discharge power

$$pda_i = \frac{\frac{SOC_k - 40}{100} \cdot bmax}{(M_{2mid} - i + 1) \cdot \Delta t} \qquad (3)$$

$$bp_i = \begin{cases} Pl_i - Ps_i - (midSch - 5), \\ \qquad\qquad\qquad\qquad Pl_i - Ps_i - pda_i > midSch \\ pda_i, \qquad\qquad\qquad Pl_i - Ps_i - pda_i \geq 0 \\ Pl_i - Ps_i, \qquad\qquad Pl_i - Ps_i - pda_i < 0 \end{cases}$$

(iv) If $20 < SOC_i \leq 40$, activate the discharging and charging process based on the current system status:

$$bp_i = \begin{cases} Pl_i - Ps_i - (midSch - 5), & discharging \\ & when\ Pl_k - Ps_k > midSch \\ Pl_i - Ps_i - (midSch + 10), & charging \\ & when\ Pl_i - Ps_i \leq midSch - 10 \\ 0, & idle\ when\ else \end{cases}$$

(v) If $SOC_i \leq 20$, only activate the charging process when $Pl_i - Ps_i \leq midSch - 20$,

$$bp_i = Pl_i - Ps_i - (midSch + 10);$$

else, the BESS is kept in passive mode;

(vi) Update $midSch$;

(vii) Set $i = k + 1$; then go back to (ii) until $i = M_{2mid}$

C. On-Peak Operation: Model Predictive Control (MPC) Method

In our previous work [8], we used model predictive control (MPC) algorithm to minimize the total electricity cost by adding the $onSch$ constraint on the on-peak demand for the entire on-peak rate periods. A brief review of our previous work is presented below:

At each time slot $i = k$:

$$minimize\ \boldsymbol{price}_i \cdot \boldsymbol{pex}_i \cdot \Delta t$$
$$subject\ to\ bc_i = bc_{i-1} - bp_i \cdot \Delta t$$
$$0 \leq \boldsymbol{bp}_i \leq pda_i$$
$$bc_{min} \leq \boldsymbol{bc}_i \leq bc_{max}$$
$$pex_i = \boldsymbol{Pl}_i - \boldsymbol{Ps}_i + \boldsymbol{bp}_i$$
$$\boldsymbol{pex}_i \leq onSch$$

price is the TOU rate schedule;

pex represents the power from external grid/utility to the building;

pda is the average discharging power over the entire on-peak period;

bc is the battery capacity, where bc_{min} and bc_{max} is the minimal (20-40% SOC) and maximal (90% SOC) battery capacity;

The battery operation vector is then calculated as:

$$\boldsymbol{bp} = \begin{bmatrix} \boldsymbol{bp}_1(1) \\ \boldsymbol{bp}_2(1) \\ \vdots \\ \boldsymbol{bp}_{M_{on}}(1) \end{bmatrix}$$

For Constant Threshold MPC (CT-MPC), $\boldsymbol{bp}$ is utilized for each control slots; while for Adjusting Demand Threshold MPC (ADT-MPC), not only the $\boldsymbol{bp}$ is utilized, but the deviation between actual SOC change and the predicted change (ΔSOC) is tracked to online adjust the $onSch$. To track the ΔSOC, we used Δpd_i, the predicted discharging power at $i+1$, and the descending control horizon,

$$\Delta SOC_i = \sum_{j=t}^{k} \Delta SOC(j) = [1 \quad \ldots \quad 1]_{(k-t+1)\times 1} \cdot (\boldsymbol{bp}(t:k)$$
$$- \Delta \boldsymbol{pd}(t:k)) \times \frac{\Delta t}{bc_{max}/100}$$

when $\Delta SOC_i \leq \varepsilon$,

$$onSch_i = \max(\max(pex), onSch_{i-1} - \frac{\Delta SOC}{100} \cdot \frac{bc_{max}}{k-t+1}$$

where t is the last time slot when $onSch$ changes, and ε is a factor for the time and range of the deviation to change $onSch$. As shown in Figs. 2 and 3, if $|\varepsilon|$ is small, the algorithm reacting to system dynamics changes more quickly and vice versa. Meanwhile a large $|\varepsilon|$ increases the time to adjust to a new threshold which uses more battery capacity to maintain the previous low load.
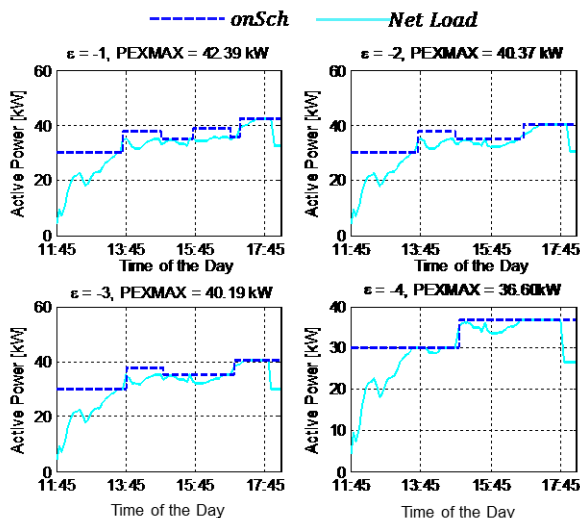

Figure 2. Net Load and $onSch$ Comparison between Different ε
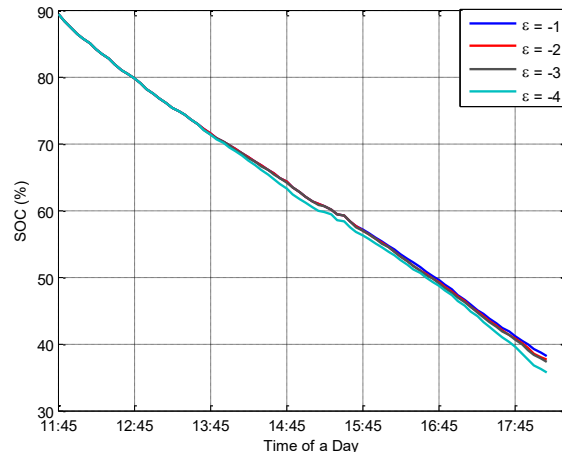

Figure 3. Battery SOC Comparison between Different ε

The CT-MPC method can maintain a stable predetermined on-peak threshold $onSch$ when the building load and solar generated power are stable; while the ADT-MPC method can adjust $onSch$ online within a microgrid system when the building load or solar generation are both unpredictable. It is obvious that the influence of inconsistent solar generation and building load during winter on-peak rate period (17:00 – 21:00, after business hours and sunset) is insignificant compared to summer on-peak rate period (12:00 – 18:00) conditions. Therefore, the CT-MPC control operation is applied to winter on-peak time, and ADT-MPC is applied to summer on-peak time. In both of the MPC control methods, only short period of historical data of building load data and solar power generation are needed to build the initial forecast models.

D. Real-time Battery Control Scheme for Conseuctive Days

In the real-time operation, the control scheme continuously and autonomously runs every 5 minutes throughout each day. The predefined $offSch$, $midSch$, and $onSch$ are initialized every month. The time indicator instructs the control scheme to use the corresponding TOU rate period operation strategy. During workdays of the week, the control scheme goes over all three different operation modes; and during weekend days and holidays, the control scheme only runs the off-peak operation and remains passive when the BESS is fully charged.

III. RESULTS OF THE REAL-TIME BATTERY CONTROL SCHEME

A. Simulation for Off-Peak Operation

Fig.4 shows a simulation result for off-peak control when the building load is higher than its normal consumption. To maintain the low $offSch$, the actual charging power is lower than the desired charging power in the first hour. The $offSch$ adjusted rapidly to ensure the full capacity at the end of the off-peak period. During the next few hours, the battery is charged relatively stable around the desired power. The proposed off-peak operation can then maintain the off-peak demand to be 92.25 kW.
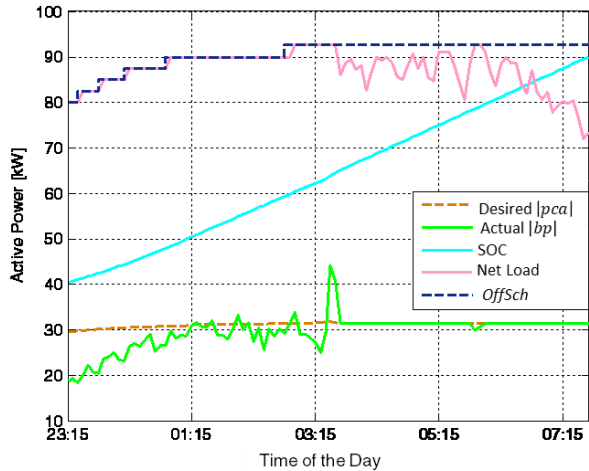
Figure 4.   Off-Peak Simulation under a High Off-Peak Load Day

B. Simulation for On-Peak Operation

During summer rate period, the microgrid encounters more system uncertainties due to the intermittent solar generation and unpredictable building load. While short term of historical data may affect the selection of initial *onSch* threshold or/and mismatched solar generation/building load profile. As shown in Fig. 5, the solar and building data is from a cloudy/rainy working day. Different initial on-peak thresholds are chosen. It is obvious that a small initial threshold results in a quick response time, while acquires more battery capacity. A better choice of the initial *onSch* inevitably performs better result, but the difference of the maximum net load between different initial thresholds is small. Therefore, the on-peak operation can always maintain the relatively minimal energy consumption and net load demand without comprehensive prior knowledge of the system.
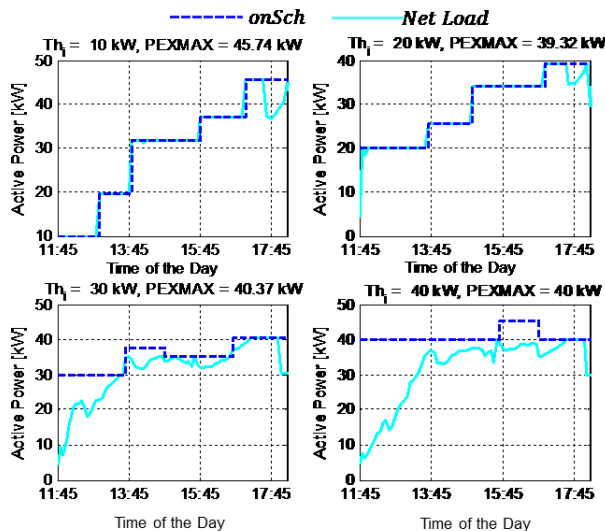

Figure 5.   Different Choice of Initial *OnSch*

C. One-day Experiment

Fig. 6 shows the results of a full-day experiment using the proposed control scheme, conducted on a regular working Tuesday. The three different shaded areas show the three different rate periods during a 24-hour period. The predetermined demand values for this day were $offSch = 90$ kW, $midSch = 60$ kW and $onSch = 30$ kW, $\varepsilon = -3$. From the graph, it can be observed that the battery was charged during the off-peak period and then discharged during the on-peak and the second mid-peak periods. Due to the sufficient solar generation in the midday, the BESS was capable of maintaining the minimal electricity consumption (near 0 kW) from the grid. At the end of the on-peak period, the SOC of the BESS was around 60%. This remaining battery capacity could then be utilized during the second mid-peak period to further reduce electricity demand and energy use. For each rate period, the net demand was tightly kept below the scheduled demand values, and the BESS was fully utilized during the operation.
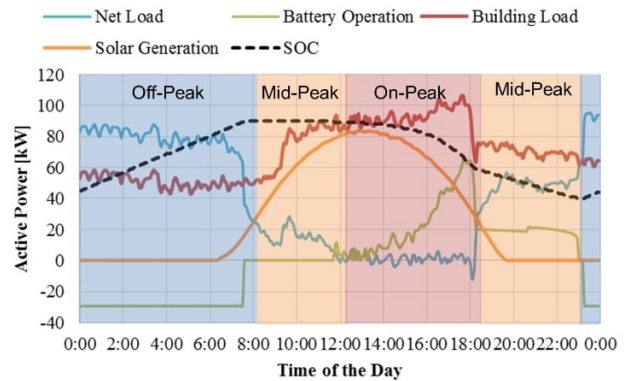

Figure 6.   Battery Control Method Experiment

IV.   SYSTEM COST EFFICIENCY

In this section, we compare electricity cost for four different system topologies:

- System 1 – the building with the solar PV system and the BESS under the proposed control scheme.
- System 2 – the building with the solar PV system and the BESS under schedule operation (one practical approach to operate the BESS with daily charging and discharging cycling without prior knowledge of the system):
  - Summer: the BESS charged at -35 kW for the first four off-peak hours, and -30 kW for the remaining off-peak hours; discharged at 40 kW during on-peak hours;
  - Winter: the BESS charged at -30 kW during off-peak hours; discharged at 60 kW for the first two on-peak hours, and 40 kW for the remaining hours.
- System 3 – the building only with the solar PV system.
- System 4 – the building only without solar or BESS.

The electricity cost is calculated based on the RPU's TOU rate schedule, and the savings between System 1 and other systems are demonstrated in Tables I and II. The electricity cost for System 1 is calculated based on the experiments conducted at the SIGI microgrid for the months of May and June. The electricity cost for other systems are numerically

calculated based on the actual solar generation and building load over the same period.

During the month of May, due to lower solar generation output and relatively stable load profiles during the on-peak periods, scheduled battery control achieves higher cost savings than the scheduled operation in the summer month of June, as seen in Table I. Therefore, the cost difference between System 1 and System 2 is smaller than the one for June in Table II. In the winter season, the BESS is mostly in passive monitoring mode during the mid-peak periods. The difference between System 1 and System 2 for the mid-peak period demand costs is equal to 0. The on-peak demand cost savings from System 1 are significant in comparison with System 3. This is due to the fact that during the on-peak period in winter, the solar generation diminishes to zero, therefore, the demand reduction is mainly accomplished by the BESS. When comparing System 1 with System 4, most energy savings originate from the renewable solar PV generation. The on-peak demand savings account for about 35.93% of the total savings.

Due to the large solar generation in the month of June, the energy stored in the BESS from the off-peak time is mostly sent back to the external grid during the on-peak hours for System 2, as seen in Table II. The overall energy (kWh) consumed by System 2 is larger than System 3 due to the energy loss during charging and discharging process. Therefore, the energy cost savings achieved by System 1 vs. System 2 is larger than System 1 vs. System 3. It is evident from the 'Peak Demand (kW) Savings' column of Table II that with the proposed battery control scheme of System 1, the peak demand reduced for all three rate periods in contrast to System 2. When compared with System 3, the largest portion of savings are obtained from the on-peak demand reduction. In addition, the energy cost savings are achieved by the shift of energy use with the operation of the BESS charging during off-peak hours and discharging during on-peak and mid-peak hours. The biggest cost difference is between System 1 and System 4. Solar panels produce large amount of electrical energy, and most of the energy savings are derived from solar generation. The other important savings component stem from the reduction of peak demand, and approaches about 31.32% of the total savings.

TABLE I.   MAY (WINTER MONTH) ELECTRICITY COST COMPARISON FOR DIFFERENT SYSTEM ARCHITECTURES

System Comparison	Energy (kWh) Savings ($)	Peak Demand (kW) Savings ($)			Total ($)
		On Peak	Mid Peak	Off Peak	
System 1 vs. System 2	84.26	59.5	0	14.6	158.36
System 1 vs. System 3	97.44	472.3	24.84	-24.7	594.58
System 1 vs. System 4	953.7	585.65	115.44	-24.7	1630.09

TABLE II.   JUNE (SUMMER MONTH) ELECTRICITY COST COMPARISON FOR DIFFERENT SYSTEM ARCHITECTURES

System Comparison	Energy (kWh) Savings ($)	Peak Demand (kW) Savings ($)			Total ($)
		On Peak	Mid Peak	Off Peak	
System 1 vs. System 2	209.65	105.92	17.24	6.19	339.00
System 1 vs. System 3	104.38	381.12	17.24	-33.10	469.64
System 1 vs. System 4	1182.82	584.56	126.26	-27.21	1866.43

V.   CONCLUSIONS

With the combination of three different rate period control strategies, an easy implementable, low complexity real-time control scheme is developed and deployed for the SIGI microgrid system. The proposed control scheme can maintain load demands for different rate periods in a low range and efficiently utilize the capacity of the battery, while prolonging the lifetime of the battery system. By comparing this control scheme with three other different system configurations, the systems with the BESS can always achieve higher electricity cost savings than the system without it. Furthermore, operating the BESS in the proposed real-time control schemes can generate additional cost savings, and achieve significant electricity cost reduction under the TOU rate schedule.

REFERENCES

[1] EPA (United States Environmental Protection Agency): Centralized Generation of Electricity and its Impacts on the Environment [Online]. Available: https://www.epa.gov/energy/centralized-generation-electricity-and-its-impacts-environment .

[2] R. H. Lasseter and P. Paigi, "Microgrid: a conceptual solution," 2004 IEEE 35th Annual Power Electronics Specialists Conference (IEEE Cat. No.04CH37551), Aachen, Germany, 2004, pp. 4285-4290 Vol.6.

[3] Feng, W., Jin, M., Liu, X., Bao, Y., Marnay, C., Yao, C., & Yu, J. (2018), "A review of microgrid development in the United States – A decade of progress on policies, demonstrations, controls, and software tools," in Applied Energy, 228, 1656–1668.

[4] "Schedule TOU Large General And Industrial Service," City of Riverside Public Utilies Department [Online]. Available: https://www.riversideca.gov/utilities/pdf/2015/Electric%20Schedule%20TOU%20-%20Effective%2007-1-15%20TES%20Removed.pdf

[5] H. Kanchev, D. Lu, F. Colas, V. Lazarov and B. Francois, "Energy Management and Operational Planning of a Microgrid With a PV-Based Active Generator for Smart Grid Applications," in IEEE Transactions on Industrial Electronics, vol. 58, no. 10, pp. 4583-4592, Oct. 2011.

[6] C. Chen, S. Duan, T. Cai, B. Liu and G. Hu, "Smart energy management system for optimal microgrid economic operation," in IET Renewable Power Generation, vol. 5, no. 3, pp. 258-267, May 2011. P. Sreedharan, J. Farbes, E. Cutter, C.K. Woo, J. Wang, "Microgrid and renewable generation integration: University of California, San Diego", in Applied Energy, vol 169, pages 709-720, Feb. 2016.

[7] "WB-LYP1000AHC," Winston Battery, [Online]. Available: http://en.winston-battery.com/index.php/products/power-battery/item/wb-lyp1000ahc?category_id=176. [Accessed 21 09 2017].

[8] X. Yun, M. Todd, S. Ula, M. J. Barth and A. A. Martinez-Morales, "A Comparison Between Two MPC Algorithms for Demand Charge Reduction in a Real-World Microgrid System," in 43rd IEEE Photovoltaic Specialists Conference, Portland, 2016.